Multiple Wave Diffraction Anomalous Fine Structure

Yen-Ru Lee,[1] Yuri P. Stetsko,[1,2] Wen-Hsien Sun,[1] Shih-Chang Weng,[1] Shen-Yuan Cheng,[1] Guin-Gi Lin,[1] Yun-Liang Soo,[1] and Shih-Lin Chang[1,2,*]

[1]*Department of Physics, National Tsing Hua University, Hsinchu, Taiwan, Republic of China 300*
[2]*National Synchrotron Radiation Research Center, Hsinchu, Taiwan, Republic of China 300*

(Received 19 June 2006; published 3 November 2006)

A new method, multiple-wave diffraction anomalous fine structure, combining the x-ray multiple-wave diffraction and diffraction anomalous fine structure techniques, is proposed. The real part of dispersion correction $\Delta f'$ and fine structure χ function can be obtained directly by multiple diffraction analysis without using Kramers-Krönig relations and kinematical fitting of diffracted intensity. Better wave vector sensitivity of the fine structure is expected. The multiple-wave diffraction anomalous fine structure experiment for a GaAs single crystal is reported as an example.

DOI: 10.1103/PhysRevLett.97.185502 PACS numbers: 61.10.Dp, 61.10.Ht

X-ray scattering is closely related to x-ray absorption. In principle, the scattered intensity and the absorption coefficient are linked through the real part f' and the imaginary part f'' of the anomalous scattering amplitude by the Kramers-Krönig relations [1]. The well developed extended x-ray absorption fine structure (EXAFS) and near-edge x-ray absorption fine structure (NEXAFS) provide short-range ordering structural information. This includes the near-neighbor bond lengths, and coordination number around the specifically excited absorbing atoms for EXAFS and the valence, empty orbital and bonding information for NEXAFS. On the other hand, x-ray diffraction yields long-range atomic structural information. In 1992 Stragier *et al.* [2] combined the two analysis approaches into the so-called diffraction anomalous fine structure (DAFS) method, which has become a powerful method for both short- and long-range order structure analysis of single crystals, powders, thin films, multilayers and superlattices [3–9].

The conventional DAFS measures the intensities of two-wave diffractions versus the photon energies in the vicinity of an absorption edge. The fine spectral distribution of the diffracted intensity, together with the absorption spectra, gives simultaneously atom-site and wave vector selectivities. The final goal of DAFS is to obtain site-dependent spectral distributions of f' and f'' of the excited atom. And later the fine structure function $\chi_A(E)$ versus photon energy E can be determined.

The analysis of the conventional DAFS involves the fitting of the DAFS intensity spectrum with the kinematical theory of x-ray diffraction. The accuracy of the analyzed results rely on the atomic scattering factors f' and f''. However, the f' obtained from the Hilbert transformation with the Kramers-Krönig relations for truncated measured absorption data may not be reliable. In addition, the data analysis procedure is complicated. For this reason, a new method called multiple-wave DAFS, abbreviated as MDAFS, is proposed in this Letter, where a simple analysis procedure is given and the useful phase information of the structure-factor multiplets, linking the imaginary part with the real part of the structure factors, involved in multiple diffraction is considered [10,11]. This linkage to phases thereby substitutes the Kramers-Krönig relations. Moreover, the constraint imposed by the additional reflection on the diffraction geometry makes the MDAFS a much more wave vector and site-sensitive technique than the two-wave DAFS for the measurements.

The scattering amplitude from atoms in solids consists of a smooth and an oscillating fine structures. The former is due to a bare free atom, and the latter is from the modulation caused by the scattering of photoelectrons from the surrounding atoms. The atomic scattering factor of an atom A for a given momentum transfer $\vec{q}$ and photon energy E is

$$\begin{aligned} f(\vec{q}, E) &= f_{0A}(\vec{q}) + \Delta f'_{0A}(E) + i\Delta f''_{0A}(E) + \Delta f''_{0A}(E)\chi_A \\ &= f_{0A}(\vec{q}) + f'(E) + f''(E), \end{aligned} \tag{1}$$

where $\chi_A(E) = \chi'_A(E) + i\chi''_A(E)$. The first three terms on the right of the first equation are the contributions from the bare atom, where f_{0A} is the normal atomic scattering factor, and $\Delta f'_{0A}$ and $\Delta f''_{0A}$ the real and the imaginary dispersion corrections. The last term $f''(E)$ of the second equation, analogous to EXAFS, is related to the oscillating fine structure χ_A function, whose real χ'_A and the imaginary part χ''_A can be defined, from (1), as

$$\begin{aligned} \chi'_A(E) &= \frac{\Delta f'_{\mathrm{exp}}(E) - \Delta f'_{0A}(E)}{\Delta f''_{0A}(E)}, \\ \chi''_A(E) &= \frac{\Delta f''_{\mathrm{exp}}(E) - \Delta f''_{0A}(E)}{\Delta f''_{0A}(E)}, \end{aligned} \tag{2}$$

where $\Delta f'_{\mathrm{exp}}$ and $\Delta f''_{\mathrm{exp}}$ are the anomalous dispersion corrections that can be obtained from DAFS and EXAFS measurements, respectively.

The diffracted intensity of a Bragg reflection G, as in the kinematical approach, is proportional to the square of the structure factor, defined as [5,6]

$$F(\vec{q}_G, E) = F_{0G} e^{i\delta_{0G}} + \sum_{j=1}^{N_A} \Delta f''_{0A} |\alpha_{A_j}| e^{i\delta_{A_jG}} \chi_{Aj}, \quad (3)$$

where the first term on the right contains the scattering of all nonresonant atoms and resonant atoms A_j. The second term is related to the fine structure resulting from all the resonant A atoms at different site j, and $\alpha_{A_j} = c_{A_j} \exp(-M_{A_j} q^2) \exp(i\delta_{A_jG})$, where c_{A_j} is the occupation factor, the probability for the resonant A atom occupying the j site. M_{A_j} is the Debye-Waller factor and phase $\delta_{A_jG} = \vec{q}_G \cdot \vec{r}_{A_j}$, $\vec{r}_{A_j}$ being the position vector of the j site in the unit cell. F_{0G}, namely, $F_{0G}(q_G, E)$, is the magnitude of the smooth complex structure factor and δ_{0G} is the phase.

The diffraction fine structure can be isolated from the experimental data by either the direct spline method or the iterative Kramer-Krönig method [3,9]. In the direct spline method, the DAFS data are splined and normalized, then the spline is removed and used as the reference. This normalized fine structure yields $\chi_{q_G}(k)$ for a given scattering vector q_G, where $k = [2m(E - E_0)]^{1/2}/\hbar$ is the modulus of the photoelectron wave vector and E_0 is the binding energy. The iterative Kramer-Krönig method finds a pair of $\Delta f'$ and $\Delta f''$, which give the best fit to the measured intensity data. Iteration by using the $\Delta f'$ and $\Delta f''$ values of Refs. [12,13] as starting values is necessary to find a correct pair. However, for a noncentrosymmetric structure, the iterative Kramers-Krönig procedure cannot be applied.

Multiple diffraction occurs when several sets of atomic planes in a crystal are simultaneously brought into position to diffract an incident wave. For a three-wave (O, G, L) diffraction, the crystal is first aligned for the primary reflection G and then rotated around the reciprocal lattice vector $\vec{q}_G$ of the G reflection, the so-called azimuth Ψ scan, to bring the additional set of planes of the secondary reflection L to also satisfy Bragg's law. Hence, three reciprocal lattice points O, G, and L are situated on the surface of the Ewald sphere, where point O stands for the incident wave. With this azimuthal Ψ rotation around $\vec{q}_G$, the secondary reflection L interferes with the primary G reflection via the coupling reflection $G - L$. Because of this interference the intensity of each reflection is modified. The modified intensity of the G reflection is related to the structure-factor triplet $F_3 = F_L F_{G-L}/F_G$ and the triplet phase $\delta_3 = \delta_L + \delta_{G-L} - \delta_G$, where δ_G, δ_L, and δ_{G-L} are the individual phases of the primary and secondary and coupling reflections, respectively. These phases connect the f' and f'' via the structure factors. The triplet phase can be measured experimentally. According to the dynamical theory of x-ray diffraction, the diffracted wave field $D_G^{(3)}$ of the G reflection in the three-wave diffraction is given in an iterative Born approximation [11,14] by

$$\vec{D}_G^{(3)} = A_G \chi_G \vec{K}_G \times \vec{K}_G \Big\{ \vec{D}_0 + A_L \frac{\chi_L \chi_{G-L}}{\chi_G} \times [\vec{K}_L \times (\vec{K}_L \times \vec{D}_0)] \Big\}, \quad (4)$$

where $\vec{D}_0$ is the direct incident wave field. A_M is the resonance function for $M = G$, L [11,14], which can be represented in terms of the azimuthal rotation angle $\Delta\Psi$ and the fundamental width η of the three-wave diffraction as $1/2(\Delta\Psi) - i\eta$ [11,14,15]. The first term in (6) is the 2-wave field $\vec{D}_G^{(2)}$ and the second term is due to the interference involving the secondary and the coupling reflections. The χ_G is the electric susceptibility proportional to the structure factor of the G reflection. The quantity $(\chi_L \chi_{G-L})/\chi_G$ is proportional to structure-factor triplet: $F_3 = \Gamma_0(\chi_L \chi_{G-L})/\chi_G$, where $\Gamma_o = -r_e \lambda^2/(\pi V)$ and r_e, λ, and V are the classic radius of electron, the x-ray wavelength, and the volume of the crystal unit cell, respectively. F_3 can be represented in terms of the smooth and oscillatory parts of the MDAFS spectrum:

$$\begin{aligned} F_3 = {} & F_{0G}^* F_{0L} F_{0(G-L)} e^{i\delta_{03}} \\ & + \sum_j^{N_A} f''_{0A} \alpha_{A_j} |\chi_{A_j}| [F_{0L} F_{0(G-L)} e^{i(\delta_{03} + \Delta_G - \phi_{\chi_j})} \\ & + F_{0L} F_{0G} e^{i(\delta_{03} - \Delta_{G-L} + \phi_{\chi_j})} \\ & + F_{0G} F_{0(G-L)} e^{i(\delta_{03} - \Delta_L + \phi_{\chi_j})}] \end{aligned} \quad (5)$$

where $\Delta_G = \delta_{0A} - \delta_{A_jG}$, ϕ_{χ_j} is the phase of χ_{A_j}, and δ_{03} is the triplet phase independent of χ_{A_j}. Combining Eqs. (4) and (5), we obtain the intensity variation, ΔI_G as [14]

$$\begin{aligned} \Delta I_G = \frac{I_{G(3)} - I_{G(2)}}{I_{G(2)}} &= I_K + I_D \\ &= P_{LL} \frac{1}{|\chi_G|^2} \Gamma_o^2 F_3 F_3^* + \frac{\Gamma_o}{|\chi_G|} A_L |A_G|^{-1} P_{GL} F_3 \\ &\quad + \frac{\Gamma_o}{|\chi_G|} A_L^* |A_G|^{-1} P_{GL} F_3^* \end{aligned} \quad (6)$$

where the phase-independent I_K is proportional to $F_3 F_3^*$ and the phase-dependent I_D is the sum of the second and third terms of the second equation. Therefore, I_D is given by

$$\begin{aligned} I_D \propto F_3 + F_3^* = {} & F_{0G}^* F_{0L} F_{0(G-L)} \cos(\delta_{03} + u) \\ & + \sum_j^{N_A} f''_{0A} \alpha_{A_j} [\chi_{A_j}^* F_{0L} F_{0(G-L)} \\ & \times \cos(\delta_{03} + \Delta_G + u) + \chi_{A_j} F_{OL} F_{0(G)} \\ & \times \cos(\delta_{03} - \Delta_{G-L} + u) \\ & + F_{0G} F_{0(G-L)} \chi_{A_j} \cos(\delta_{03} - \Delta_L + u)] \end{aligned} \quad (7)$$

where $\Delta_M = \delta_{0M} - \delta_{AM}$ for $M = G$, L, and $G - L$. P_{LL} and P_{GL} are the polarization factors. The ratio of the resonance functions is expressed as $A_L/|A_G| = |A_L|/|A_G| \exp(iu)$. As usual in a three-wave diffraction, I_D shows an asymmetric profile, depending on the resultant phase given in (7), while I_K forms a symmetric intensity

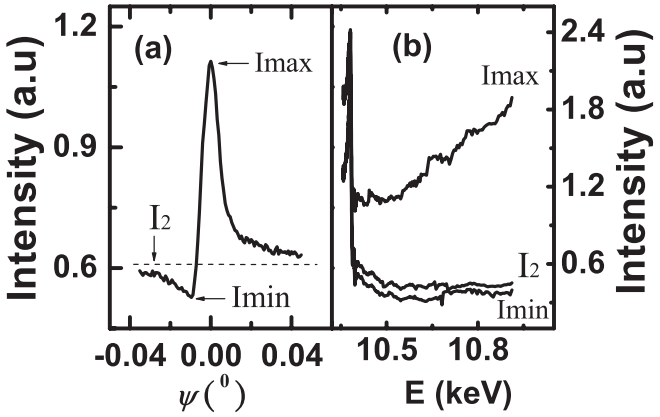

FIG. 1. (a) Measured GaAs (222) intensity versus $\Delta\Psi$ of the three-wave (000)(222)(33$\bar{1}$) diffraction position and (b) diffraction intensities at the maximum, minimum, and two-wave background of (a) versus x-ray photon energy.

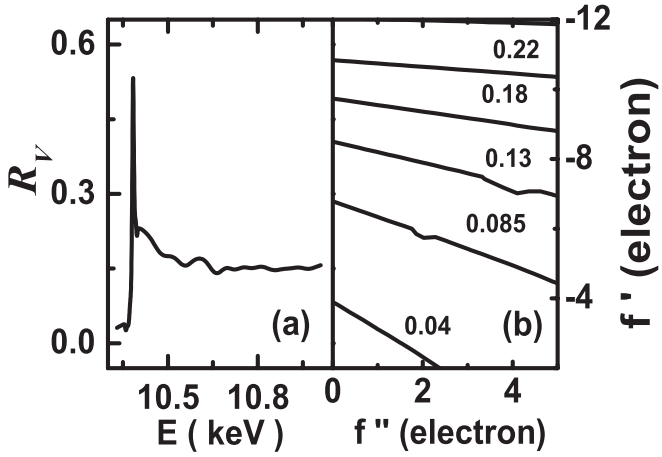

FIG. 2. (a) Measured intensity ratio R_v versus photon energy and (b) the calculated R_V versus f' and f'' for Fig. 1.

background. Both I_D and I_K are related to the fine structure χ_A. Thus, the distribution of the three-wave reflected intensity versus photon energy provides the information about the dispersion corrections $f'(E)$ and $f''(E)$. By employing the expression (6) and (7), the asymmetrical reflected intensity distribution of ΔI_G can be calculated as a function of the azimuthal angle Ψ at a specific photon energy. Following this idea, instead of intensity, we propose to use the visibility R_v as the parameter for the MDAFS spectrum. R_v, closely related to the phases mentioned, is defined as

$$R_v = \frac{I_2 - I_{\min}}{I_{\max} - I_2} \tag{8}$$

where I_2 is the two-wave intensity background and $I_{\max}$ and $I_{\min}$ are the maximum and minimum intensities of the three-wave profile [Fig. 1(a)]. The corresponding spectral distributions of $f'(E)$ and $f''(E)$ can be determined with ease.

The experiment was carried out at the wiggler beamline BL17B, National Synchrotron Radiation Research Center, Taiwan. Consider the three-wave (000)(222)(33$\bar{1}$) diffraction of GaAs (111) cut crystal, with the Ga rich surface facing the x rays. The (222) is a symmetric Bragg and (33$\bar{1}$) an asymmetric Bragg reflection. Two scintillation counters are used; one to measure the (222) diffracted intensity and the other, placed off the diffracted plane, parallel to the crystal surface, to detect the fluorescent yield. Both the MDAFS and EXAFS data can be taken simultaneously or separately. The experimental setup and conditions are the same as those for the resonance phase measurements described in [16,17]. The energy range used covers the Ga K edge and the energy resolution is about 0.2 eV. The fluorescence yield and the three-wave diffraction profile for each photon energy are measured. Figure 1(a) shows the Ψ scan for $E = 10.413$ keV above the Ga K edge, where the average background is the two-wave intensity of (222). The asymmetric profile results from the resultant phase effect. The intensities at maximum, minimum, and the two-wave background, which determine the visibility R_v of the asymmetry, are plotted against the photon energy in Fig. 1(b).

The phase dependence of R_v linking the f' and f'' makes R_v a sensitive parameter for the determination of f' and f''. Since f'' can be directly obtained from the absorption spectrum derived from the fluorescence yield after proper corrections, the corresponding f' can be estimated from the measured R_v ratio. The measured R_v ratio and f'' versus photon energy are shown in Figs. 2(a) and 3(b). With the aid of intensity calculation, the equi-intensity ratio curves of R_v for various combinations of f' and f'' are plotted in Fig. 2(b), where a smooth R_v surface has been constructed with a numerical algorithm of interpolating two-dimensional cubic splines. For a given f'' at the energy E, the f' can be easily obtained in the equi-intensity plot. The determined $f'(E)$ is shown in Fig. 3(a). The corresponding fine structure function of the real part of $\chi(k)$, deduced from Fig. 3 according to (2), is shown in the inset of Fig. 4(c). The Fourier transform of $\chi'(k)$ gives the radial

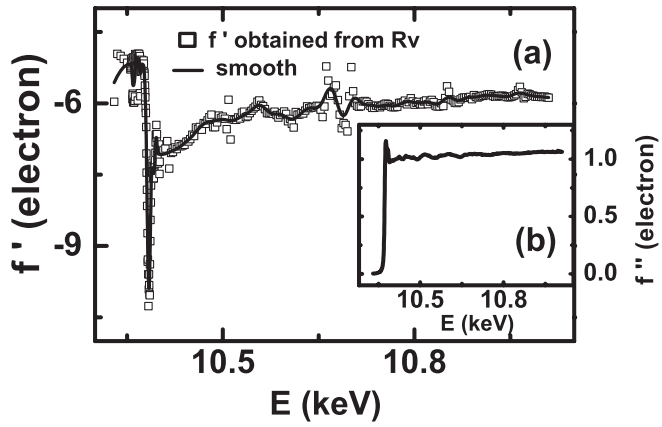

FIG. 3. Measured (a) f' and (b) f'' from the intensity ratio R_v from Fig. 1 and fluorescence yield, respectively.

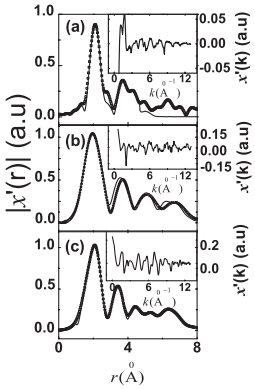

FIG. 4. The Fourier transformed $\chi'(r)$ of (a) EXAFS, (b) DAFS, (c) MDAFS signals (points), and the theoretical fit (solid curve). The insets show the background subtracted and normalized signals $\chi'(k)$.

distribution function $\chi'(r)$ shown in Fig. 4(c), which yields the distances between the central atom and other atom shells. The corresponding $\chi(k)$ and $\chi'(r)$ for EXAFS and DAFS are shown in Figs. 4(a) and 4(b). The Fourier transform of real space $\chi'_A(r)$ used is

$$\chi'_A(r) = \sum_{\Gamma,j} k_\Gamma^a \chi'_{A_j}(k_\Gamma) W_j(k) \exp\{i[2kr_{A_j}^\Gamma + \delta_{A_j}^\Gamma(k)]\}$$

where $a = 1$–3. $\delta_{A_j}^\Gamma(k)$ is the photoelectron phase shift, Γ a photoelectron scattering path, $r_{A_j}^\Gamma$ the effective path length, and $W_j(k)$ the window function. The theoretical fits to Figs. 4(a) and 4(c) are based on the program FEFF and FEFFIT [18,19]. The complex function $\chi_A(k)$ for GaAs is generated by the FEFF. The output of FEFF contains the amplitude and phase of $\chi_A(k)$, which lead to $\chi_A(k) =$ amp[FEFF]cos(phase[FEFF]). And the real part $\chi_A(k)$ is fitted by using the modified FEFFIT function. The average lattice parameter of GaAs is 5.6539 Å and the path lengths to the first and second shells are 2.476 and 4.062 Å, with the accuracies $\Delta r = 0.027$ Å for the MDAFS, 0.046 Å for DAFS, and -0.01 Å for EXAFS. A background correction of MDAFS $\chi_A(k)$ is also considered by the FEFFIT, with the goodness of fit [19], the R factor 0.025 for MDAFS, 0.049 for DAFS, and 0.043 for EXAFS. With the present experimental accuracy of DAFS and MDAFS, only the first two shells give reliable structural information.

In conclusion, we have demonstrated that using the phase information inherent in multiple diffraction provides a sensitive parameter R_v of intensity ratio for the determination of the spectral distributions of f' and f''. Moreover, the atomic site is well defined in the plane determined by the reciprocal lattice vectors of the primary and the secondary reflection. Experimentally, the samples were aligned under the multiple diffraction condition, which is more stringent and precise than in the conventional DAFS. In other words, the MDAFS is more wave vector- and site sensitive than the conventional DAFS. Also the site selectivity can be easily implemented in the input structure factors for the intensity calculation as shown in (6). For thin films and layered epitaxial materials, the Born or Bethe approximation is equally applicable to give kinematical intensity ratios R_v, which lead directly to the spectral distributions of f' and f''.

The authors are indebted to the Ministry of Education and National Science Council for the financial support.

*Electronic address: slchang@phys.nthu.edu.tw

[1] R. Krönig, J. Opt. Soc. Am. **12**, 547 (1926).
[2] H. Stragier, J. O. Cross, J. J. Rehr, L. B. Sorensen, C. E. Bouldin, and J. C. Woicik, Phys. Rev. Lett. **69**, 3064 (1992).
[3] L. Sorensen, J. Cross, M. Newville, B. Ravel, J. Rehr, H. Stragier, C. Bouldin, and J. Woicik, in *Resonant Anomalous X-ray Scattering: Theory and Applications*, edited by G. Materlik, C. Sparks, and K. Fischer (North-Holland, Amsterdam, 1994).
[4] I. J. Pickering, M. Sansone, J. Marsch, and G. N. George, J. Am. Chem. Soc. **115**, 6302 (1993).
[5] J. C. Woicik, J. O. Cross, C. E. Bouldin, and B. Ravel *et al.*, Phys. Rev. B **58**, R4215 (1998).
[6] M. G. Proietti, H. Renevier, J. L. Hodeau, J. Garcia, J. F. Berar, and P. Wolfers, Phys. Rev. B **59**, 5479 (1999).
[7] H. Renevier, J. L. Hodeau, P. Wolfers, S. Andriev, J. Weight, and R. Frahm, Phys. Rev. Lett. **78**, 2775 (1997).
[8] J. O. Cross, M. Newville, J. J. Rehr, L. B. Sorenson, C. E. Bouldin, G. Watson, T. Gouder, G. H. Lander, and M. I. Bell, Phys. Rev. B **58**, 11 215 (1998).
[9] B. Ravel, C. E. Bouldin, H. Renivier, J.-L. Hodeau, and J.-F. Berar, Phys. Rev. B **60**, 778 (1999).
[10] S.-L. Chang, *Multiple Diffraction of X-rays in Crystals* (Springer-Verlag, Berlin, 1984).
[11] S.-L. Chang and M.-T. Tang, Acta Crystallogr. Sect. A **44**, 1065 (1988).
[12] D. T. Cromer and D. Liberman, J. Chem. Phys. **53**, 1891 (1970).
[13] D. T. Cromer and D. Liberman, Acta Crystallogr. Sect. A **37**, 267 (1981).
[14] S.-L. Chang, Acta Crystallogr. Sect. A **54**, 886 (1998).
[15] K. Hümmer and H. W. Billy, Acta Crystallogr. Sect. A **42**, 127 (1986).
[16] S.-L. Chang, Y.-S. Huang, C.-H. Chao, M.-T. Tang, and Yu. P. Stetsko, Phys. Rev. Lett. **80**, 301 (1998).
[17] Yu. P. Stetsko, G.-Y. Lin, Y.-S. Huang, C.-S. Chao, and S.-L. Chang, Phys. Rev. Lett. **86**, 2026 (2001).
[18] A. L. Ankudinov, B. Ravel, J. J. Rehr, and S. D. Conradson, Phys. Rev. B **58**, 7565 (1998).
[19] J. J. Rehr and R. C. Albers, Phys. Rev. B **41**, 8139 (1990).